ACS SENSORS

pubs.acs.org/acssensors

Article

Ultrasensitive Monitoring of Museum Airborne Pollutants Using a Silver Nanoparticle Sensor Array

Zheng Li,* Zhiwei Wang, Javid Khan, Maria K. LaGasse, and Kenneth S. Suslick*

Cite This: *ACS Sens.* 2020, 5, 2783−2791

Read Online

ACCESS | Metrics & More | Article Recommendations | Supporting Information

ABSTRACT: The preservation of cultural heritage materials requires extremely low concentration limits for indoor pollutants. This poses an unmet challenge for monitoring the artwork in museums and on exhibit, especially to do so in a cost-effective manner for a large number of locations. A novel type of colorimetric sensor array based on printed inks of 10 nm silver nanoparticles (AgNPs) with several different capping agents has been developed as an alternative to metal coupons or other passive sampling indicators traditionally used by conservators. The AgNP colorimetric sensor array, combined with digital imaging, offers ultrasensitive dosimetric identification of acidic and oxidizing gases and other air pollutants commonly found in a museum; the limits of detection are sub-ppb for 1 h exposures. For an array of AgNP inks with various capping agents, a unique and distinguishable color response pattern is observed for each specific analyte. Excellent discrimination among 11 gas pollutants over a wide range of concentrations was demonstrated using standard chemometric methods. The observed changes in color during pollutant exposure originate from the sintering of solid-state nanoparticles that leads to changes in the localized surface plasmon resonance. Such chemically induced sintering mechanism of nanoparticles paves the way for a new class of field-deployable solid-state optical sensor arrays. As an example, we have demonstrated the use of AgNP sensor arrays for the nondestructive analysis of acidic volatile emission from five types of printing paper, relevant for the conservation of cultural heritage objects, including ancient manuscripts and books.

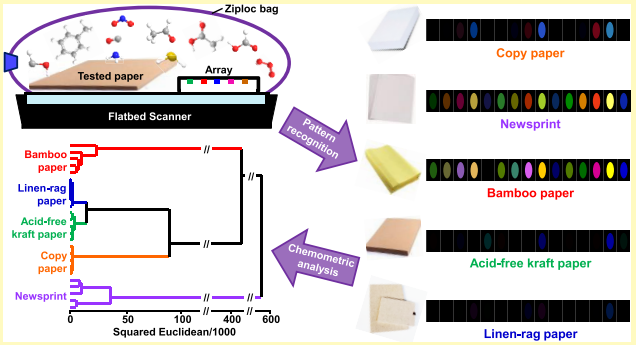

KEYWORDS: *airborne pollutants, nanoparticle sintering, nanosilver, ultrasensitive detection, colorimetric sensor array, artwork conservation*

The conservation of artwork and historical artifacts is of tremendous importance for the preservation of our cultural heritage.[1−3] Artwork protection requires monitoring and controlling the environment in which they are displayed; both physical and chemical factors, such as light, temperature, pollutants, and humidity, can have a profound impact on the long-term survival of these objects. It is seldom realized, however, how vulnerable cultural heritage objects are to airborne pollutants, either from the outside atmosphere or, even more importantly, the local microenvironment inside sealed display cases or storage areas. Indeed, for artwork, the recommended pollutant exposure levels of acids, oxidants, and aldehydes are generally at a few ppb or even sub-ppb concentrations,[4−7] which are hundreds or even thousands of times lower than the human permissible exposure limits (PELs) established by NIOSH/OSHA.[8] This is, of course, because people can heal and have finite lifetimes, in contrast to inanimate cultural relics. Consequently, there remains a pressing need for monitoring the artwork in museums or on exhibit on a regular and ongoing basis, especially to do so in a cost-effective manner for a large number of locations.

Pollution monitoring technology for conservation must be sensitive, but also cost-effective. The most common method used for the qualitative monitoring of potentially harmful airborne chemicals originating from materials used in storage, display, or transport of cultural heritage objects is the Oddy test, which was developed originally at the British Museum in the 1970s.[9] To prevent potentially harmful impact on the artwork, historic artifacts, or other cultural heritage objects, the Oddy test uses clean metal coupons (e.g., silver, copper, and lead) and visual inspection to detect pollutant hazards from materials used to construct display cases. Nevertheless, the utility of the Oddy test is severely limited even as a qualitative method by the long evaluation times required (a standard 28-day test period) and by the inconsistency of the subjective

Received: March 23, 2020
Accepted: June 18, 2020
Published: June 18, 2020

visual assessment.[10,11] Alternatively, analyte-specific indicators with passive sampling (including various indicator papers[12] and Draeger tubes[13]) are at best semiquantitative, require a new device for each analyte of interest, and are limited by the cost and sensitivity. Other detection tools, such as AirCorr monitoring systems,[14] piezoelectric quartz crystals,[15] and α-sense sensors,[16] are well established and have also been used by the cultural heritage community to evaluate the environment in storage containers, sealed frames, galleries, and storage rooms. Traditional electronic nose technology (e.g., sensor arrays based on metal-oxide or conductive polymer sensors) has had limited application to pollutant monitoring,[17,18] but museum and conservation applications are especially difficult due to their sensitivity, sensor drift, poor chemical selectivity, and interference from response to changes in ambient humidity.[19−21] More complex analytical instrumentation (e.g., gas chromatography or mass spectrometry) is generally beyond the means of conservators.

The use of colorimetric sensor arrays (CSAs) as an inexpensive "optoelectronic nose" has been developed over the past two decades[19,22−24] for the detection and identification of both individual compounds[25,26] and highly similar complex mixtures[27−30] generally at ppm to tens of ppb levels. CSA is distinct from nearly all electronic nose techniques in that the responses of sensors depend primarily on the chemical reactivity of the analytes and not their physical properties (e.g., physisorption-induced mass or volume changes in the sensors). These CSAs have relied on a diverse range of chemical interactions with chemically responsive molecular dyes, including pH indicators, solvatochromic dyes, metal-containing chromogens, redox indicators, and nucleophilic adducts.[19] Most of these interactions are reversible or at least partially reversible and do not have the capability of cumulative monitoring of pollutants.

For preservation of cultural heritage objects, time is not of the essence, and it is the long-term sensitivity of the artwork to pollutants at very low concentrations that is most important. Prior CSAs are not suitable for cumulative ultrasensitive detection.[31] This is in large part due to the continuous neutralization of acid-sensitive dye formulations by ambient CO_2, which is, of course, a weak acid present in air at high concentration (~400 ppm). In addition, there are two other disadvantages for any equilibrium-based sensor: (1) there is no improvement in sensitivity with increased dosage (i.e., exposure time) and (2) arrays must be imaged in real time. The first disadvantage is critical, where long-term, but very low concentration, exposures need to be monitored. The second disadvantage, real-time imaging, substantially complicates real-world use of sensor arrays during exhibition conditions.

Another class of colorimetric and fluorometric sensors based on metallic nanostructures, such as gold or silver nanoparticles (AgNPs), have been extensively employed for biological macromolecular analytes.[32−37] These sensors rely on changes in localized surface plasmon resonance (LSPR) as the transduction method to detect biological analytes through the induction of nanoparticle aggregation by binding of the biomolecules to specific receptors on the nanoparticles (e.g., antibodies). Similar AgNPs have also found broad applications in environmental monitoring, pharmaceutics, food safety, and security screening.[38−42] Very few attempts, however, have been made to detect small molecules in the gas phase by colorimetric changes in AgNPs, with the notable exception of the detection of H_2S[43,44] and NH_3[45] with Ag nanofilms and our own recent work on diverse analytes.[46]

In this work, we described a new class of colorimetric sensor arrays based on chemically induced sintering of printed AgNP inks.[46] We further report here the cumulative sensing properties of the newly developed sensors that are suitable for the detection, identification, and quantification of pollutants of importance to the preservation of cultural heritage objects even at sub-ppb levels. The solid-state nanoparticle sensor array is able to discriminate among 11 pollutants relevant to museum conservation at sub-ppm concentrations with high accuracy. We expect that this new sensor array will find a useful place as a much more powerful alternative to the traditional Oddy test[9] and other currently used methods for the monitoring of potential airborne pollutants in passive sampling environments (as discussed earlier).

EXPERIMENTAL SECTION

Reagents and Materials. All reagents and materials were of analytical-reagent grade and were used without further purification. Cetrimonium bromide (CTAB), polyvinylpyrrolidone (PVP, average M_w ~29 000), cysteine, dodecanethiol, $AgNO_3$, $NaBH_4$, and all solvents were purchased from Sigma-Aldrich (St. Louis, MO); polypropylene membrane (Product #PP021605820) was purchased from Sterlitech Corporation (Kent, WA); sensor cartridges were custom injection-molded from low-volatility polycarbonate (Dynamic Plastics, Chesterfield Township, MI). Paper materials were purchased from local grocery stores.

Synthesis of AgNP Inks. A 30 mL aqueous solution of $AgNO_3$ (0.10 M) was combined with 25 mL of xylene containing a phase transfer catalyst, CTAB (0.40 M), and vigorously stirred for 0.5 h. The organic phase was isolated from the aqueous phase, and 0.36 g of cysteine or 0.61 g of 1-dodecanethiol or 0.34 g of PVP was added. After the mixture was stirred for 15 min, the silver ions were reduced by 20 mL of an aqueous solution of $NaBH_4$ (0.30 M) and then stirred for 12 h. The organic phase was isolated from the aqueous phase, and the nanoparticles were washed in ethanol and acetone to remove the residual phase transfer catalyst and unbound thiol in the organic phase. The concentration of Ag nanoparticles in the as-synthesized AgNP inks was determined by inductively coupled plasma atomic emission spectroscopy (ICP-OES) (2.3 ± 0.2 mM). The resultant products were diluted with xylene to different degrees for printing.

Sensor Array Preparation. The linear colorimetric sensor arrays were printed using a robotic pin printer commercially available from ArrayIt Inc., as per the details elsewhere.[25,31,46,47] Fifteen sensor elements from three sets of AgNP inks were printed on a polypropylene membrane at 3 mm center−center distance using an array of stainless steel rectangular pins. The arrays were dried under vacuum for 1 h at room temperature after printing and stored in heat-sealed and N_2-filled aluminized Mylar bags before any measurement was performed.

Gas Analyte Generation and Measurement. Gas analyte streams containing the chosen analyte concentrations were prepared by mixing the prediluted analyte stream with dry and wet filtered air using a series of MKS digital mass flow controllers (MFCs) to reach specific analyte concentrations at 50% relative humidity (RH). Before each calibration, the gas flow was run for 30 min to achieve a stabilized concentration; for calibration, analyte concentrations were measured using the in-line FTIR analysis with an MKS Multigas Analyzer (model 2030). For the collection of sensor array responses in a passive environment (inside a 22 L polypropylene Ziploc bag (70 × 50 cm) filled with gas analytes at a fixed concentration), sensor array images were captured every 5 min using an Epson 600 flatbed scanner, while the arrays were exposed to the target analyte at 0, 0.125, 0.25, 0.5, 1, and 2 ppm in 50% RH filtered air for 1 h. Sensor images were collected at 300 dpi and saved as bmp files to the PC terminal. RGB data were initially saved in a 12-bit color space for all

https://dx.doi.org/10.1021/acssensors.0c00583
ACS Sens. 2020, 5, 2783−2791

of the 15 sensor elements and then converted to an 8-bit color space for ΔRGB analysis. The flatbed scanner was calibrated using a one-time measurement of a 0% reflectance standard (i.e., a blackening sensor substrate) and a 100% reflectance standard (i.e., a blank sensor substrate).

Database Analysis. Two unsupervised statistical methods, principal component analysis (PCA) and hierarchical cluster analysis (HCA), were performed for database clustering using MVSP software (Kovach Computing Services, Pentraeth, Isle of Anglesey, U.K.); in all cases, minimum variance (i.e., "Ward's Method") was used for HCA clustering. For quantitative cross-validation, predictive classification was carried out using the support vector machine (SVM) analysis with custom software that makes use of an open-source SVM library, LIBSVM, using a linear kernel with default parameters.[48]

Calculation of Limits of Detection (LODs). The LODs for relevant gases were determined from multipoint data by plotting LOD = $3*N*[A]/(S_A - S_C)$ vs concentration (in ppb), where $[A]$ is the analyte concentration in ppb, N is the noise determined from multiple images of the same array, S_A is the Euclidean distance (ED) of the most responsive spot after a 1 h exposure to analyte, and S_C is the ED of the same spot after a 1 h exposure to the control. A first-order polynomial fit was used to determine the LOD as $[A]$ approached the LOD. Sensor responses of five representative pollutants (SO_2, H_2S, HCO_2H, CH_3CO_2H, and HCHO) between 0.125 and 2 ppm were collected for 1 h exposures.

Alternatively, one may extrapolate LODs from a single data point by simply taking the observed ED value of the most responsive sensor spot after a 1 h exposure at 1 ppm concentration and dividing that into three times the noise observed for the same spot after 1 h in a control experiment. A comparison of LODs calculated by these two methods gives very similar results. Comparisons of the sensor array LODs to OSHA/NIOSH permissible exposure limits (PELs) and to the recommended culture heritage collection exposures are given in Table 1.

Table 1. LODs Obtained by the Cumulative Sensor Array Compared to Human Permissible Exposure Limits (PELs) and Suggested Concentration Limits for Cultural Heritage Materials of Critical Museum Pollutants[a]

pollutants	LODs from single-point data (ppb*h)	human PELs[b] (ppb)	suggested limits for collections[c] (ppb)
SO_2	0.28	2000	<2
H_2S	0.49	10 000	<0.1
HCO_2H	0.47	5000	<20
CH_3CO_2H	0.92	10 000	<280
HCHO	1.3	750	<20
O_3	0.61	100	<5
NO_2	0.34	5000	<10

[a]LODs were calculated based on the 1 h measurement of museum pollutants. [b]NIOSH permissible exposure limits (PELs) are given as a time-weighted average, 8 h/day. [c]Grzywacz, C. M. Monitoring for Gaseous Pollutants in Museum Environments; Getty Publications, 2006.

RESULTS AND DISCUSSION

Development of Printable Ag Nanoparticle Inks. AgNPs were synthesized via a template-free method as mentioned in our prior work,[46] which enables the deposition of AgNP dispersions on hydrophobic substrates. AgNPs were functionalized with three different capping agents to make three different inks: polyvinylpyrrolidone (PVP)-capped, AgNP-A; cysteine-capped, AgNP-B; and dodecanethiol-capped, AgNP-C (Supporting Information or SI, Figure S1a). The choice of these capping agents diversifies the chemical reactivity of the AgNPs so as to assist in the array recognition of molecular analytes at the nanoparticle surface. The stabilities of these AgNP inks are excellent, with no apparent aggregation or precipitation after storage for over 6 months.

Optimization of AgNP-Based Solid-State Sensor Array. The as-synthesized AgNP inks were diluted to a series of concentrations (19, 29, 33, 38, and 51 nM of total Ag atom concentration) and printed on hydrophobic polypropylene membranes; AgNPs were deposited on the porous substrate as bar-shaped sensor elements ("spots") with distinctive colors after solvent evaporation (SI Figure S1b). The printing of hydrophobic inks on hydrophobic membranes minimizes the potential interference from ambient humidity during sensor measurement.

The sensor response to the exposure of analytes in a passive sampling environment is highly dependent on the AgNP concentration in the inks used for printing (SI Figure S2). With too high of a AgNP concentration in the ink (e.g., >2 mM in total Ag atom concentration), no color change is observable upon analyte exposure, simply because the spot is essentially opaque (SI Figure S2); with too low of a concentration of AgNP, there are too few nanoparticles present to induce sufficient spot color or color changes (e.g., <20 nM; SI Figure S2). The five representative dilutions of each capped Ag ink were selected and incorporated in the linearized sensor array for gas pollutant measurements (Figure 1a).

The color changes of the printed AgNP spots in the sensor array (i.e., changes in the RGB values) originate from red shifts of the plasmon bands upon analyte exposure, as seen in the diffuse reflectance spectra of the printed AgNP sensors (SI Figure S3). These red shifts are primarily attributed to the extrinsic size effects originating from the AgNP aggregation in the printed spots (as discussed later), which behave similarly to colloidal AgNPs in solution.[49]

Gas-Sensing Properties of the AgNP-Based Sensor Array. The array response to 11 common museum pollutants was measured all at 1 ppm and repeated in quintuplicate; color difference profiles are displayed in Figure 1a. The readily distinguishable patterns for each of the 11 pollutants are observed in the color changes of the array during exposure. The intensity of color change of any given sensor spot is dependent on (1) the chemical properties of the analytes, (2) the initial ink concentration used for printing, and (3) the choice of the capping agent used for the AgNP inks. The most responsive sensor spots were printed from inks with a total Ag atom concentration of ∼29 nM, and the order of responsiveness increases slightly as the capping agent is changed from PVP to cysteine and to dodecanethiol. The newly designed sensor array has proven notably nonresponsive to common potential interferents (Figure 1), including ethanol, methanol, ethyl acetate, benzene, and acetonitrile at 1 ppm, as well as the weak acid CO_2 even at 20-fold of its ambient level (i.e., 8000 ppm).

Sensing mechanisms have been summarized in our prior work,[46] which is associated with metallic nanoparticle sintering in the presence of gaseous chemicals with different chemical properties. On exposure to more corrosive analytes (i.e., acids and oxidants), loss of surface capping ligands is more likely to occur due to their protonation or oxidation; AgNPs are much more prone to agglomeration even in the solid state[50] if capping agents are partially stripped from the core of AgNPs, as has also been reported for silver nanoparticles in acidic or

https://dx.doi.org/10.1021/acssensors.0c00583
ACS Sens. 2020, 5, 2783−2791

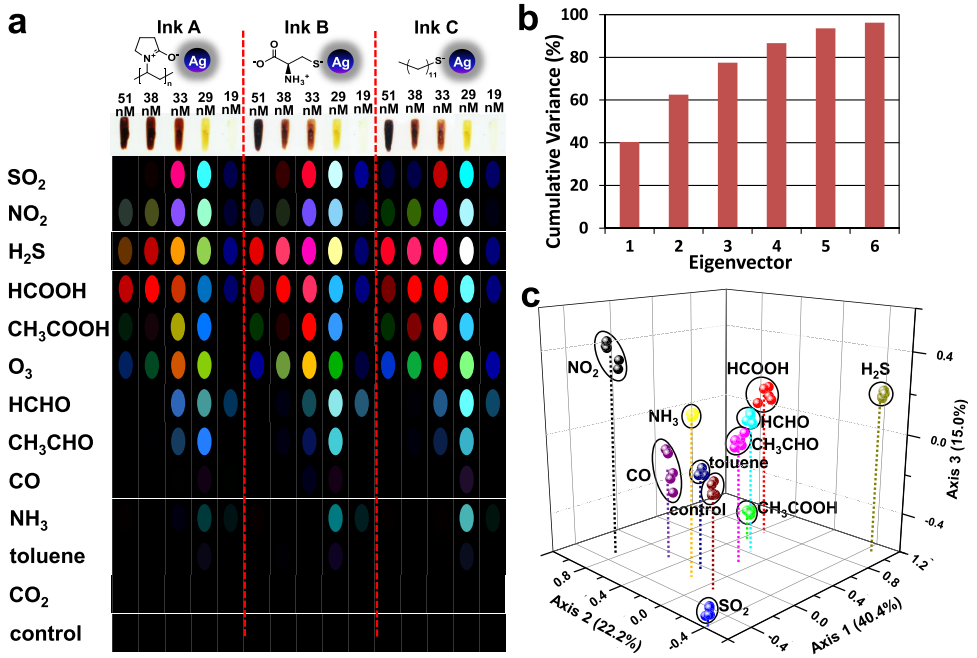

Figure 1. AgNP sensor responses and chemometric analysis. (a) Sensor array responses to 11 gas pollutants at 1 ppm, CO_2 at 8000 ppm, and comparison to a control (i.e., filtered air). The patterns shown represent the color change upon exposure to analytes as the change in RGB values of each AgNP printed spot. Each gas is premixed with wet N_2 to 50% relative humidity, and each color difference pattern is the average of quintuplicate trials for a 1 h exposure. For display purposes, the color range is expanded from 3 to 8 bits per color (i.e., the RGB color range of 3−10 was expanded to 0−255). Spots 1, 6, and 11 were generated from the printing of AgNP inks with 51 nM of total Ag atom concentration; spots 2, 7, and 12 from 38 nM; spots 3, 8, and 13 from 33 nM; spots 4, 9, and 14 from 29 nM; and spots 5, 10, and 15 from 19 nM. (b) PCA scree plot shows that six dimensions are needed to capture 95% of the total variance. (c) PCA score plot of the 11 gas pollutants at 1 ppm plus a control; the three dimensions plotted only encompass ∼78% of the total variance.

oxidizing solutions.[51,52] On exposure to less reactive gas analytes (i.e., CO, NH_3, and toluene), only small color changes were observed from the array, which may be ascribed to the nonspecific interactions (i.e., physical or chemical adsorption) that occurred at the AgNP−gas interface that can modestly affect the absorbance band of the AgNPs.

Chemometric Analysis of Sensor Responses. The pattern of the colorimetric response of the 15 different AgNP sensors in the array provides a facile means to differentiate one analyte from another and one concentration of an analyte from another concentration. To evaluate quantitatively the ability of the array to discriminate among the types of gas pollutants and their concentrations, several chemometric analyses (specifically, hierarchical cluster analysis (HCA), principal component analysis (PCA), and support vector machine (SVM) analysis)[53−55] were performed on the collected colorimetric sensing data. HCA and PCA are both unsupervised exploratory data analyses, i.e., "clustering" techniques: HCA is commonly used to evaluate the dissimilarity among data points and cluster them in a multivariate vector space, while PCA is to estimate the dimensionality of the data and attempts to project the data into a minimized number of dimensions.

The HCA dendrogram of 11 pollutants at 1 ppm concentration and a control (clean air) in quintuplicate trials is shown in Figure S4. The cluster discrimination among analytes is excellent. The clusters representing toluene and NH_3 are relatively close, largely due to the weak and nonspecific interactions involved for those two analytes. The PCA scree plots for the library of 11 pollutants (Figure 1b) show that six dimensions are required to describe 95% of the total variance; traditional electronic nose technologies typically require only one or two (or occasionally three) dimensions to capture 95% of the variance. For colorimetric sensor arrays, however, six dimensions are a relatively low dimensionality,[19] which is due in large part to the limited chemical diversity of analytes used in these studies. The PCA score plot (Figure 1c) based on the top three principal components is still useful for visualization and presents similar excellent clustering results, even though only ∼75% of the total variance is captured in those three dimensions.

For clustering among analytes at different concentrations, analysis techniques that handle high-dimensional data are preferred: HCA for clustering analysis and SVM for quantitative prediction. Further studies were made among the four acidic gases at five different concentrations (ranging from 2 ppm to 125 ppb for a 1 h passive exposure). Good discrimination among these analyte/concentration ranges was observed in the HCA dendrogram (SI Figure S5a), with an error rate <4% (i.e., four misclusterings out of 105 trials in total): due to the resemblance of formic and acetic acids, a supercluster is formed for those two analytes and four errors were observed among their different concentrations (e.g., misclustering between 250 ppb HCO_2H and 500 ppb CH_3CO_2H), which are still fully separable from all concentrations of H_2S or SO_2. Similar PCA analysis of the same data gives good clustering as well and confirms the observed dimensionality of the data set (SI Figure S5b,c).

For comparison, SVM analysis offers a supervised and more quantitative method for data classification and prediction, i.e., identifying new entries into a known and predetermined data set of different analyte classes. SVM generates an algorithm to

https://dx.doi.org/10.1021/acssensors.0c00583
ACS Sens. 2020, 5, 2783−2791

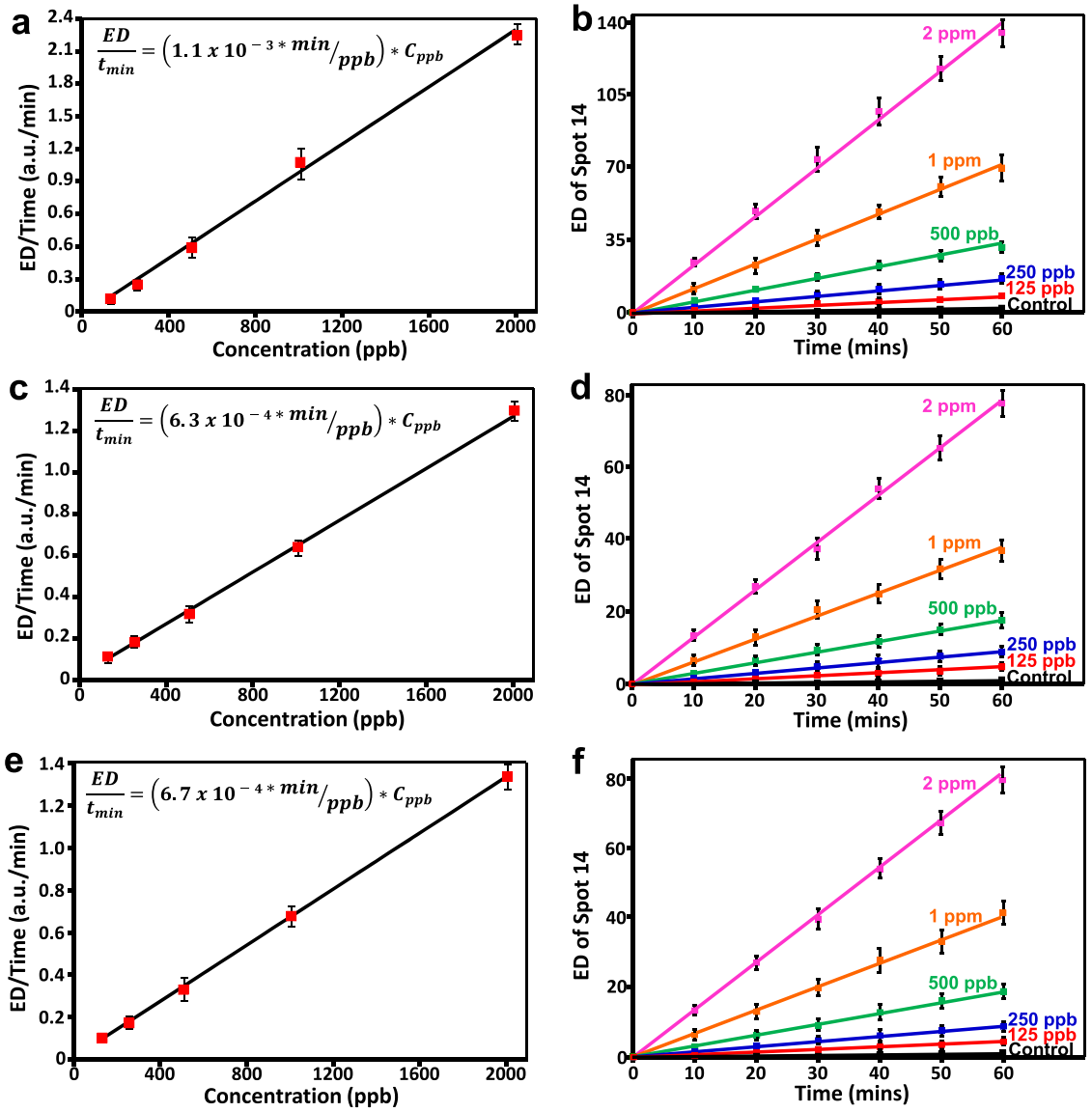

Figure 2. Calibration curve plotting the Euclidean distance of spot #14 (i.e., most responsive single sensor, as highlighted in Figure 3) per time (ED/time) vs vapor concentration or time of (a, b) SO_2, (c, d) H_2S, and (e, f) HCO_2H for a 1 h passive sampling. Each gas is premixed with wet N_2 to reach 50% relative humidity, and each error bar represents 2σ (standard deviation) from five independent trials. The equation in each chart is taken from a least-squares linear fit and can be used to determine the time-weighted average concentration from the data collected in field trials. LODs were determined from the concentration corresponding to 3N, where N is the noise determined in control experiments, as given in Table 1.

compare an unknown analyte to an established library of known analytes and is standard for the analysis of complex multidimensional data, e.g., face and voice recognition.[56,57] SVM relies on pairwise class prediction and focuses on the data most likely to be misclassified (i.e., data vectors near the decision boundary of any given pairwise class, known as "support vectors") to create optimized decision boundaries that best separate the data for each given pair of classes in multidimensional space. The results of SVM analysis using a standard leave-one-out permutation model are shown in SI Tables S1−S4: all 11 pollutants give perfect classification, and all concentrations of acidic gases show very good grouping results, with only two errors from CH_3CO_2H at 500 ppb and one from HCO_2H at 250 ppb; i.e., the overall cross-validation accuracy is >99% among the types of pollutants and > 97% among concentrations.

In addition to the quantification or classification of individual reactive gases, our sensor array was also effective in discriminating gas mixtures. As shown in Figure S6, patterns of binary or ternary mixtures between SO_2, HCO_2H, and HCHO are distinctive; HCA results demonstrate that the clusters belonging to each analyte label are well separated from each other.

Quantification of Pollutants. The response of the AgNP-based sensor array to these pollutants is essentially irreversible and linearly cumulative (Figure 2) as a function of both the time and concentration. We have previously shown that our prior colorimetric sensor arrays[19,22] (made mostly of organic dyes and metalloporphyrins) are generally mostly reversible. The drawback of sensor reversibility is that there is no improvement in the overall sensitivity with increased dosage. For monitoring the microenvironment of cultural heritage objects (e.g., the artwork inside display cases), the response

https://dx.doi.org/10.1021/acssensors.0c00583
ACS Sens. 2020, 5, 2783−2791

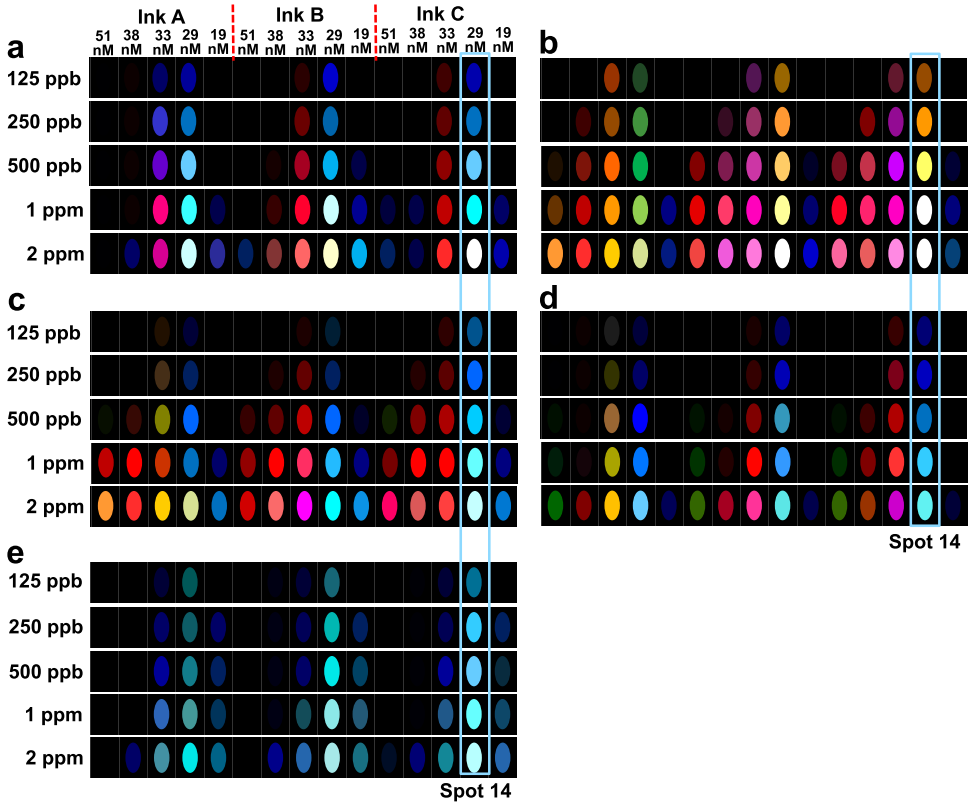

Figure 3. Averaged array response to (a) SO_2, (b) H_2S, (c) HCO_2H, (d) CH_3CO_2H, and (e) HCHO at five vapor concentrations ranging from 0.125 to 2 ppm for a 1 h passive sampling. Each gas is premixed with wet N_2 to reach the specific analyte concentration at 50% relative humidity, and each color different pattern is the average of five independent trials. For display purposes, the color range is expanded from 3 to 8 bits per color (i.e., the RGB color range of 3−10 was expanded to 0−255). Spot 14 is the single most responsive AgNP sensor element.

time is a relatively noncritical issue: daily or even weekly monitoring is generally sufficient. The AgNP-based array is ideally suited to long exposure times and can permit the ultrasensitive detection of pollutant analytes down to sub-ppb level by extending the exposure period from several minutes to hours or even a few days.

To examine the use of AgNP sensor arrays for quantification of different pollutants, we collected sensor responses of five representative pollutants (SO_2, H_2S, HCO_2H, CH_3CO_2H, and HCHO) between 0.125 and 2 ppm for 1 h exposures; each concentration of each analyte produces a unique color difference pattern (Figure 3). These responses (defined by the Euclidean distance of the color differences of all sensor spots) increase essentially linearly as a function of the exposure time (Figure 2 and SI Figure S7): the AgNP sensor arrays are dosimetric and cumulative in their quantification of analytes. This is consistent with the sintering process responsible for the colorimetric response, as discussed above. The dosimetric feature of the sensor array was further validated by the extended exposure to high and low concentrations of SO_2 on the time frames of minutes up to several days (SI Figure S8): response curves of the sensors are linear before becoming saturated at sufficient dosage. Sensor exposures at high concentrations (>0.3 ppm) lead to relatively fast response and dose-dependent saturation (as seen clearly in SI Figure S8 for exposures at 10, 2, and 0.5 ppm); for low concentrations (<0.15 ppm), the response rate of the sensor is proportionally slower and permits the quantitative monitoring of air pollutants over a week. Response profiles collected at different pollutant concentrations are fully consistent with the dosimetric (cumulative) nature of the sensor array.

Table 1 lists the sensor array's limits of detection (LODs) for critical museum pollutants and compares these LODs to the respective OSHA/NIOSH PELs[8] and to the suggested exposure limits for cultural heritage collection materials.[6] These LODs are determined from the most sensitive spot (i.e., spot #14) as a function of the analyte concentration for passive exposure for 1 h. The AgNP sensor array generally shows sub-ppb LODs for 1 h exposures, which are well below their respective PELs (typically by more than a 1000-fold) and generally below even the suggested exposure limits for cultural heritage materials. We note that these LODs can be pushed even lower simply by extending the total exposure time, given the linearity of the cumulative response of these AgNP arrays. A comparison to the typical exposure indicators (e.g., Draeger tubes) that are in current use in museum environments[12,31] is provided in SI Table S5: dramatic improvements in sensitivities are noted, even when passive exposure with the AgNPs is compared to active (i.e., pumped) exposure with Draeger tubes. In comparison to the traditional Oddy tests, the AgNP sensors are much faster (1 h compared to often a week or more for the Oddy test) and quantitative (which Oddy tests are not). We note as well that other forms of digital imaging can be used in place of the ordinary flatbed scanners: we have previously used digital cameras, cell phone cameras, and contact image sensors (e.g., business card scanners) successfully with colorimetric sensor arrays.[26]

Sensor Array for Detection of Acidic Volatiles and Discrimination among Types of Paper. Old books

https://dx.doi.org/10.1021/acssensors.0c00583
ACS Sens. 2020, 5, 2783−2791

normally give off a complex chemical bouquet of odors due to slow but continuous decomposition of active components in the paper, a process that can be autocatalytic through the effects of the acidic volatiles so produced. Detecting early signs of acidic paper degradation products would prove useful guidance for preservation efforts. Paper is made primarily of cellulose, many natural plant components, as well as specific chemical additives and chemical processing that improve the paper's physical properties.[58] Cellulose is inherently resistant to aging, but the other components (e.g., lignin) or additives can be vulnerable to degradation by heat, humidity, and UV light. Before the 19th century, paper was made mostly of cotton and linen rags, relatively pure forms of cellulose that are free of unstable additives.[59] Starting from the late 1840s, paper stock was switched to cheaper and more readily available wood-pulp fibers, which contain residues of lignin, hemicelluloses, and other components from pulping and bleaching processes. These components tend to produce acidic products that trigger even faster degradation of paper, especially under sunlight or on exposure to oxygen in air.

In the second half of the 20th century, alkaline paper became increasingly common[60] with the shift in the main filler material from kaolin clay to precipitated calcium carbonate in the pulp; this required the pulp and sizing to be chemically neutralized typically with calcium bicarbonate. Such alkaline paper has expected lifetimes of 500−1000 years.[61]

We tested the sensor array against volatiles released from five different types of printing paper during the short-term storage in a closed container of air (~22 L) and under normal indoor light condition (fluorescent lamp, ~30 W) for 12 h, as a means of nondestructive analysis. As shown in Figure 4a, 10 pages of each type of paper (A4 size, 21 × 29.7 cm, 3.2−5.5 g/sheet) were stacked and fixed in a polyethylene Ziploc bag at a distance of 5 cm from the sensor array. Response patterns of the sensor array were collected after 12 h (Figure 4b). The array responses for each type of paper were distinct from one another (Figure 4b,c) and largely dependent on the content of acidic components in the paper.

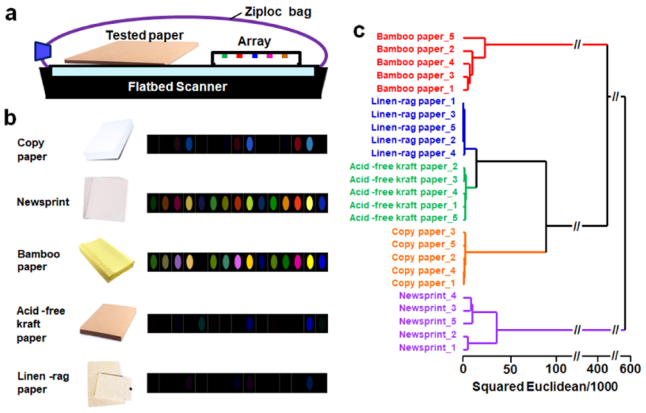

Figure 4. Sensor array detection of acidic volatiles from five different papers. (a) Experimental setup for imaging of the colorimetric sensor array during exposure to gas pollutants in a passive sampling environment (a sealed polypropylene bag filled with air and the emitted volatiles from the enclosed 10 sheets of paper) using real-time imaging with an ordinary flatbed scanner. (b) Color difference profiles of volatiles emitted from five different paper materials; each pattern is averaged out of five independent trials. For display purposes, the color range is expanded from 3 to 8 bits per color (i.e., the RGB color range of 3−10 was expanded to 0−255). (c) HCA dendrogram from quintuplicate trials, each for five types of commercial paper.

Acid-free kraft paper and linen-rag paper that contain more neutral or alkaline ingredients barely emit any corrosive volatiles to react with the array, even after 12 h exposure; as listed in Table 1, the LODs for acidic volatiles are <1 ppb*h. In contrast, newsprint and bamboo papers each produced a much greater colorimetric response in the sensor array. This reflects the much higher level of acids in the pulp fibers and oxidizing agents used during their preparation. For relatively pure commercial copy paper, only a moderate amount of corrosive gases are released, presumably from the lower level of residual bleach or other additives involved in papermaking. We measured the pH values of the testing atmosphere using a water-saturated pH indicator paper, which shows distinctive levels of acids among five paper materials after an exposure period of 12 h: pH values of newsprint (4.5) and bamboo paper (4.0) are lower than those of copy paper (6.5), kraft paper (7.0), or linen-rag paper (7.0). This result is consistent with the intensity of sensor signals as observed in Figure 4b.

The SVM cross-validation results show a clear, error-free classification of the array responses to all five paper types with quintuplicate replicates of each (Table S6). This test demonstrates that the sensor array can easily and quickly be used to determine the extent of acidic emissions from a small amount (30−50 g) of paper samples and to potentially provide a quantitative measure of the extent of degradation of paper materials according to their formulation, fabrication process, production age, and storage condition. With the further optimization in sensor composition, sampling protocol, and imaging device, this technique may well find real use for the preservation of paper containing cultural heritage objects, ranging from ancient books and manuscripts to artwork on paper or other potentially acidic media. For artwork preservation in sealed microenvironments during storage or display, the ability to make rapid assessment of their volatile emission profiles meets a real need in the conservation community.

CONCLUSIONS

We have created a disposable colorimetric sensor array for rapid, ultrasensitive, and quantitative identification of 11 common pollutants relevant to the protection of cultural heritage objects and museum environmental monitoring. This new use of capped silver nanoparticles for the dosimetric detection and quantification of small-molecule pollutants represents a substantial improvement over the traditional monitoring techniques used by art conservators. With sub-ppb sensitivities under passive exposure, these silver nanoparticle-printed sensor arrays will prove useful for evaluation of threats to artwork both within their own microenvironments during the exhibition and in storage; ready analysis by digital imaging makes analysis possible on site. Using disposable arrays of AgNP printed from inks with different capping agents and at different silver concentrations, unique and distinguishable color difference patterns for each analyte are created during exposure that are dependent on the chemical properties of the analytes (e.g., acidity, redox, etc.). Excellent discrimination among the types and concentrations of gas pollutants was achieved using standard chemometric analysis (hierarchical cluster, principal component, and support vector machine analyses).

https://dx.doi.org/10.1021/acssensors.0c00583
ACS Sens. 2020, 5, 2783−2791

The mechanism for the AgNP response to analytes originates primarily from chemically induced nanoparticle sintering, which induces particle agglomeration and consequent changes in localized surface plasmon resonance. This remarkable feature of nanoparticle sintering opens a new class of solid-state nanosensors. The nanoparticle sensor arrays have been used successfully and quantitatively to identify and distinguish the acidic volatiles emitted from a wide range of different types of commercial papers, which could potentially serve as a useful supplement to other available techniques for nondestructive analysis of cultural heritage materials, such as old books, manuscripts, or artwork.

■ ASSOCIATED CONTENT

Supporting Information

The Supporting Information is available free of charge at https://pubs.acs.org/doi/10.1021/acssensors.0c00583.

Sensor array design, pattern response data, spectroscopic results, PCA, HCA, and SVM analyses, and quantification of LODs achieved during passive sampling with the colorimetric sensor array (PDF)

■ AUTHOR INFORMATION

Corresponding Authors

Zheng Li − *Institute for Advanced Study, Shenzhen University, Shenzhen, Guangdong 518060, P. R. China;* orcid.org/0000-0001-9066-5791; Email: zhengli24@szu.edu.cn

Kenneth S. Suslick − *Department of Chemistry, University of Illinois at Urbana—Champaign, Urbana, Illinois 61801, United States;* orcid.org/0000-0001-5422-0701; Email: ksuslick@illinois.edu

Authors

Zhiwei Wang − *Institute for Advanced Study, Shenzhen University, Shenzhen, Guangdong 518060, P. R. China*

Javid Khan − *Institute for Advanced Study, Shenzhen University, Shenzhen, Guangdong 518060, P. R. China*

Maria K. LaGasse − *Department of Chemistry, University of Illinois at Urbana—Champaign, Urbana, Illinois 61801, United States*

Complete contact information is available at: https://pubs.acs.org/10.1021/acssensors.0c00583

Notes

The authors declare no competing financial interest.

■ ACKNOWLEDGMENTS

This work was supported by the Initial Scientific Research Fund of Young Teachers in Shenzhen University (No. 000002110553), the Guangdong Joint Fund of Fundamental and Applied Research (No. 2019A1515110242), and the Guangdong University Young Talents Project (No. 2019KQNCX127).

■ REFERENCES

(1) Brimblecombe, P. *The Balance of Environmental Factors Attacking Artifacts*; Wiley: Chichester, 1994.

(2) Whitmore, P. M. *Conservation Science Research: Activities, Needs, and Funding Opportunities*; National Science Foundation, 2005.

(3) Di Turo, F.; Proietti, C.; Screpanti, A.; Fornasier, M. F.; Cionni, I.; Favero, G.; De Marco, A. Impacts of air pollution on cultural heritage corrosion at European level: What has been achieved and what are the future scenarios. *Environ. Pollut.* **2016**, *218*, 586−594.

(4) Tétreault, J. Agent of Deterioration: Pollutants. In *Agents of Deterioration*; Elsevier, 2013.

(5) ASHRAE, 2019. https://www.ashrae.org/technical-resources/ashrae-handbook/table-of-contents-2019-ashrae-handbook-hvac-applications.

(6) Grzywacz, C. M. *Monitoring for Gaseous Pollutants in Museum Environments*; Getty Publications, 2006.

(7) Hatchfield, P. B. *Pollutants in the Museum Environment: Practical Strategies for Problem Solving, Exhibition and Storage*; Archetype Publications, 2002.

(8) NIOSH. *Pocket Guide to Chemical Hazards*; DHHS (NIOSH): Washington, DC, 2007.

(9) Oddy, W. A. An unsuspected danger in display. *Mus. J.* **1973**, *73*, 27−28.

(10) Bamberger, J. A. Comments on an improved Oddy test using metal films. *Stud. Conserv.* **2012**, *57*, 187−188.

(11) Wang, S.; Kong, L.; An, Z.; Chen, J.; Wu, L.; Zhou, X. An Improved Oddy Test Using Metal Films. *Stud. Conserv.* **2011**, *56*, 138−153.

(12) Grzywacz, C. M.; Stulik, D. C.*Passive Monitors for the Detection of Pollutants in Museum Environments*; American Institute for Conservation of Historic and Artistic Works: Albuquerque, New Mexico, 1991.

(13) Draeger_Co, 2018. https://www.draeger.com/Library/Content/tubeshandbook_br_9092086_en.pdf.

(14) Kouril, M.; Prosek, T.; Scheffel, B.; Degres, Y. Corrosion monitoring in archives by the electrical resistance technique. *J. Cult. Herit.* **2014**, *15*, 99−103.

(15) Cavicchioli, A.; Neves, C. A.; Paiva, R. I.; de Faria, D. L. A. An upgraded automatic piezoelectric quartz crystal dosimeter for environmental monitoring in indoor cultural heritage conservation areas. *Sens. Actuators, B* **2014**, *190*, 1014−1023.

(16) Patel, H. K. *The Electronic Nose: Artificial Olfaction Technology*; Springer: New Delhi, India, 2014; pp 207−241.

(17) Zampolli, S.; Elmi, I.; Ahmed, F.; Passini, M.; Cardinali, G. C.; Nicoletti, S.; Dori, L. An electronic nose based on solid state sensor arrays for low-cost indoor air quality monitoring applications. *Sens. Actuators, B* **2004**, *101*, 39−46.

(18) Veríssimo, M. I. S.; Oliveira, J. A. B. P.; Evtuguin, D. V.; Gomes, M. T. S. R. Preserve Your Books through the Smell. *ACS Sens.* **2019**, *4*, 2915−2921.

(19) Askim, J. R.; Mahmoudi, M.; Suslick, K. S. Optical sensor arrays for chemical sensing: the optoelectronic nose. *Chem. Soc. Rev.* **2013**, *42*, 8649−8682.

(20) Röck, F.; Barsan, N.; Weimar, U. Electronic Nose: Current Status and Future Trends. *Chem. Rev.* **2008**, *108*, 705−725.

(21) Diehl, K. L.; Anslyn, E. V. Array sensing using optical methods for detection of chemical and biological hazards. *Chem. Soc. Rev.* **2013**, *42*, 8596−8611.

(22) Lim, S. H.; Feng, L.; Kemling, J. W.; Musto, C. J.; Suslick, K. S. An optoelectronic nose for the detection of toxic gases. *Nat. Chem.* **2009**, *1*, 562−567.

(23) Rakow, N. A.; Suslick, K. S. A colorimetric sensor array for odour visualization. *Nature* **2000**, *406*, 710−713.

(24) Li, Z.; Askim, J. R.; Suslick, K. S. The Optoelectronic Nose: Colorimetric and Fluorometric Sensor Arrays. *Chem. Rev.* **2019**, *119*, 231−292.

(25) Li, Z.; Fang, M.; LaGasse, M. K.; Askim, J. R.; Suslick, K. S. Colorimetric Recognition of Aldehydes and Ketones. *Angew. Chem., Int. Ed.* **2017**, *56*, 9860−9863.

(26) Li, Z.; Li, H.; LaGasse, M. K.; Suslick, K. S. Rapid Quantification of Trimethylamine. *Anal. Chem.* **2016**, *88*, 5615−5620.

(27) Li, Z.; Suslick, K. S. Portable Optoelectronic Nose for Monitoring Meat Freshness. *ACS Sens.* **2016**, *1*, 1330−1335.

(28) Carey, J. R.; Suslick, K. S.; Hulkower, K. I.; Imlay, J. A.; Imlay, K. R.; Ingison, C. K.; Ponder, J. B.; Sen, A.; Wittrig, A. E. Rapid identification of bacteria with a disposable colorimetric sensing array. *J. Am. Chem. Soc.* **2011**, *133*, 7571−7576.

(29) Suslick, B. A.; Feng, L.; Suslick, K. S. Discrimination of complex mixtures by a colorimetric sensor array: coffee aromas. *Anal. Chem.* **2010**, *82*, 2067−2073.
(30) Zhang, Y.; Askim, J. R.; Zhong, W.; Orlean, P.; Suslick, K. S. Identification of pathogenic fungi with an optoelectronic nose. *Analyst* **2014**, *139*, 1922−1928.
(31) LaGasse, M. K.; Li, Z.; Khanjian, H.; Schilling, M.; Suslick, K. S. Colorimetric Sensor Arrays: Development and Application to Art Conservation. *J. Am. Inst. Conserv.* **2018**, *57*, 127−140.
(32) De, M.; Rana, S.; Akpinar, H.; Miranda, O. R.; Arvizo, R. R.; Bunz, U. H. F.; Rotello, V. M. Sensing of proteins in human serum using conjugates of nanoparticles and green fluorescent protein. *Nat. Chem.* **2009**, *1*, 461.
(33) Le, N. D. B.; Yesilbag Tonga, G.; Mout, R.; Kim, S.-T.; Wille, M. E.; Rana, S.; Dunphy, K. A.; Jerry, D. J.; Yazdani, M.; Ramanathan, R.; Rotello, C. M.; Rotello, V. M. Cancer Cell Discrimination Using Host−Guest "Doubled" Arrays. *J. Am. Chem. Soc.* **2017**, *139*, 8008−8012.
(34) Chen, G.; Roy, I.; Yang, C.; Prasad, P. N. Nanochemistry and Nanomedicine for Nanoparticle-based Diagnostics and Therapy. *Chem. Rev.* **2016**, *116*, 2826−2885.
(35) Padmos, J. D.; Personick, M. L.; Tang, Q.; Duchesne, P. N.; Jiang, D.-e.; Mirkin, C. A.; Zhang, P. The surface structure of silver-coated gold nanocrystals and its influence on shape control. *Nat. Commun.* **2015**, *6*, No. 7664.
(36) Young, K. L.; Ross, M. B.; Blaber, M. G.; Rycenga, M.; Jones, M. R.; Zhang, C.; Senesi, A. J.; Lee, B.; Schatz, G. C.; Mirkin, C. A. Using DNA to Design Plasmonic Metamaterials with Tunable Optical Properties. *Adv. Mater.* **2014**, *26*, 653−659.
(37) Avella, M.; Cocca, M.; Errico, M. E.; Gentile, G. *Nanotechnological Basis for Advanced Sensors*; Reithmaier, J. P.; Paunovic, P.; Kulisch, W.; Popov, C.; Petkov, P., Eds.; Springer: Dordrecht, 2010; pp 511−517.
(38) Lai, J.; Niu, W.; Luque, R.; Xu, G. Solvothermal synthesis of metal nanocrystals and their applications. *Nano Today* **2015**, *10*, 240−267.
(39) Lewandowski, W.; Fruhnert, M.; Mieczkowski, J.; Rockstuhl, C.; Górecka, E. Dynamically self-assembled silver nanoparticles as a thermally tunable metamaterial. *Nat. Commun.* **2015**, *6*, No. 6590.
(40) Rycenga, M.; Cobley, C. M.; Zeng, J.; Li, W.; Moran, C. H.; Zhang, Q.; Qin, D.; Xia, Y. Controlling the Synthesis and Assembly of Silver Nanostructures for Plasmonic Applications. *Chem. Rev.* **2011**, *111*, 3669−3712.
(41) Stark, W. J.; Stoessel, P. R.; Wohlleben, W.; Hafner, A. Industrial applications of nanoparticles. *Chem. Soc. Rev.* **2015**, *44*, 5793−5805.
(42) Ando, J.; Asanuma, M.; Dodo, K.; Yamakoshi, H.; Kawata, S.; Fujita, K.; Sodeoka, M. Alkyne-Tag SERS Screening and Identification of Small-Molecule-Binding Sites in Protein. *J. Am. Chem. Soc.* **2016**, *138*, 13901−13910.
(43) Chen, R.; Morris, H. R.; Whitmore, P. M. Fast detection of hydrogen sulfide gas in the ppmv range with silver nanoparticle films at ambient conditions. *Sens. Actuators, B* **2013**, *186*, 431−438.
(44) Chen, R.; Whitmore, P. M. *Science and Function of Nanomaterials: From Synthesis to Application*; Harper-Leatherman, A. S.; Solbrig, C. M., Eds.; American Chemical Society, 2014; pp 107−120.
(45) Rithesh Raj, D.; Prasanth, S.; Vineeshkumar, T. V.; Sudarsanakumar, C. Ammonia sensing properties of tapered plastic optical fiber coated with silver nanoparticles/PVP/PVA hybrid. *Opt. Commun.* **2015**, *340*, 86−92.
(46) Li, Z.; Suslick, K. S. Chemically Induced Sintering of Nanoparticles. *Angew. Chem., Int. Ed.* **2019**, *58*, 14193−14196.
(47) Li, Z.; Suslick, K. S. Colorimetric Sensor Array for Monitoring CO and Ethylene. *Anal. Chem.* **2019**, *91*, 797−802.
(48) Chang, C.-C.; Lin, C.-J. LIBSVM: A Library for Support Vector Machines. *ACM Trans. Intell. Syst. Technol.* **2011**, *2*, 1−27.
(49) Mogensen, K. B.; Kneipp, K. Size-Dependent Shifts of Plasmon Resonance in Silver Nanoparticle Films Using Controlled Dissolution: Monitoring the Onset of Surface Screening Effects. *J. Phys. Chem. C* **2014**, *118*, 28075−28083.
(50) Wagle, D. V.; Baker, G. A. Cold welding: a phenomenon for spontaneous self-healing and shape genesis at the nanoscale. *Mater. Horiz.* **2015**, *2*, 157−167.
(51) Axson, J. L.; Stark, D. I.; Bondy, A. L.; Capracotta, S. S.; Maynard, A. D.; Philbert, M. A.; Bergin, I. L.; Ault, A. P. Rapid Kinetics of Size and pH-Dependent Dissolution and Aggregation of Silver Nanoparticles in Simulated Gastric Fluid. *J. Phys. Chem. C* **2015**, *119*, 20632−20641.
(52) Dement'eva, O. V.; Rudoy, V. M. Polishing and cold welding of gold nanoparticles under the action of Fenton's reagent. *Colloid J.* **2015**, *77*, 276−282.
(53) Cristianini, N.; Shawe-Taylor, J.*An Introduction to Support Vector Machines and other Kernel-Based Learning Methods*; Cambridge University Press, 2000.
(54) Hair, J. F.; Black, B.; Babin, B.; Anderson, R. E.; Tatham, R. L. *Multivariate Data Analysis*, 6th ed.; Prentice Hall: New York, 2005.
(55) Janata, J. *Principles of Chemical Sensors*, 2nd ed.; Springer: New York, 2009.
(56) Askim, J. R.; Li, Z.; LaGasse, M. K.; Rankin, J. M.; Suslick, K. S. An optoelectronic nose for identification of explosives. *Chem. Sci.* **2016**, *7*, 199−206.
(57) Li, Q.; Gu, Y.; Jia, J. Classification of Multiple Chinese Liquors by Means of a QCM-based E-Nose and MDS-SVM Classifier. *Sensors* **2017**, *17*, 272−286.
(58) Daniels, V. D. The chemistry of paper conservation. *Chem. Soc. Rev.* **1996**, *25*, 179−186.
(59) Hunter, D.*Papermaking*; Dover Publications: New York, 1974.
(60) Teygeler, R. *Managing Preservation for Libraries and Archives: Current Practice and Future Development*; Feather, J., Ed.; Ashgate: Aldershot, 2004; pp 83−112.
(61) Manglik, S. Role of acid-free paper in libraries: A survey. *Int. J. Libr. Inf. Sci.* **2014**, *6*, 19−21.

https://dx.doi.org/10.1021/acssensors.0c00583
ACS Sens. 2020, 5, 2783−2791